Applied Catalysis A: General 391 (2011) 205–214

Contents lists available at ScienceDirect

Applied Catalysis A: General

journal homepage: www.elsevier.com/locate/apcata

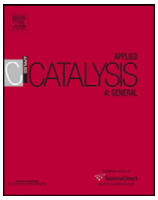

Oxidative coupling of methane over Ca- and alkali metal-doped ThO_2

Tinku Baidya, Niels van Vegten, Yijiao Jiang, Frank Krumeich, Alfons Baiker*

Institute for Chemical and Bioengineering, Department of Chemistry and Applied Biosciences, ETH Zurich, Hönggerberg, Wolfgang Pauli Strasse 10, HCI, CH-8093 Zürich, Switzerland

ARTICLE INFO

Article history:
Received 11 January 2010
Received in revised form 19 March 2010
Accepted 25 March 2010
Available online 1 April 2010

Keywords:
Thoria
Ca and alkali metal doping
Oxidative coupling of methane
Oxide ion vacancy
Oxide ion radical

ABSTRACT

$Th_{0.8}Ca_{0.2}O_{2-\delta}$ and Na/K dispersed $Th_{0.8}Ca_{0.2}O_{2-\delta}$ catalysts, synthesized by the citric acid gel method, have been tested concerning their efficiency in the oxidative coupling of methane. The structural properties of the catalysts were characterized by BET, XRD, Raman, TEM, TPD, and EPR techniques. The presence of oxide ion vacancies due to Ca ion incorporation into ThO_2 lattice was evidenced by Raman spectroscopy. EPR revealed the formation of radical oxygen in the Ca-doped ThO_2 sample after oxygen treatment at 500 °C. $Th_{0.8}Ca_{0.2}O_{2-\delta}$ showed high catalytic activity reaching about 24% methane conversion (rate: $2.3\,\mathrm{mol\,g^{-1}\,h^{-1}}$) at 56% selectivity toward C_{n+} products at 600 °C, whose performance is comparable to that of the well known Sr doped La_2O_3 catalyst. Other reference catalysts like 1.9%Mn–4%Na_2WO_4/SiO_2 and 5%Li/MgO showed considerably lower activity under these conditions. The high catalytic activity and selectivity of the Ca-doped sample is likely due to formation of stable active $\dot{O}^-$ species in the oxide ion vacancy site in the lattice.

1. Introduction

Oxidative coupling of methane (OCM) with molecular oxygen to produce higher hydrocarbons has been a topic of research since the last three decades. A wide variety of metal oxides, mainly alkali, alkaline-earth and rare earth oxides and to a minor extent transition metal oxide based catalysts, have been studied [1–6]. Sr(Ca)/La_2O_3, Li/MgO and Mn/Na_2WO_4/SiO_2 have emerged as most promising catalysts for OCM reactions, exhibiting both relatively high activity and selectivity to coupling products (C_{2+}) [7–18]. Mn/Na_2WO_4/SiO_2 showed a single-pass C_{n+} yield of more than 20% above 800 °C. Ba–La_2O_3 has been reported to give a C_{2+} yield of 18% [19]. However, the rate of methane conversion, selectivity to C_{2+} products needs to be improved and the operating temperature lowered to make this process commercially viable. Therefore, considerable effort has been invested into the development of new catalysts that work at lower temperature and show a higher C_{2+} yield.

The primary and most important step in this reaction is the homolytic abstraction of hydrogen from the methane molecule by oxygen to produce a methyl radical that combines in the gas phase with another methyl radical or hydrocarbon, yielding higher hydrocarbons [8,20–22]. Mechanistic studies have identified two possible active oxygen species, namely: (i) molecular species such as, O_2^{2-} for lanthanide oxides [22,23], and (ii) dissociated oxygen species such as nucleophilic ions $\dot{O}^-$ of the catalyst lattice [8,24,25].

Hence, the goal is to tailor the chemical properties of the lattice to facilitate the formation of these oxygen species and simultaneously to enhance their migration in the lattice. Doped rare earth oxides are more active as OCM catalysts than other group of metal oxides [3]. For example, the origin of high OCM activity of La_2O_3 and its doped analogues is due to facile oxygen migration in the lattice [26–28]. As a general concept, p-type conductivity of the oxide lattice has been considered responsible for higher OCM activity. Rare earth oxides have high p-type conductivity and this property is well correlated to the C_2 formation activity in the series of rare earth oxides with the OCM activity decreasing from lanthanum to lutecium, i.e. corresponding to decreasing oxygen activation capability [18]. Anshits et al. summarized the importance of defects in a number of systems and demonstrated their crucial role in the doped Bi_2O_3 system [29]. Creation of oxide ion vacancies by doping with foreign cations is considered to increase the hole concentration in an irreducible oxide and transform it to a p-type semiconductor with increase in oxygen partial pressure, according to the following scheme: $V_0 + O_2 \Leftrightarrow 2\dot{O}^- + 2h^+$. However, activity and selectivity of these oxides are strongly dependent on the lattice type of the oxide. Thus, according to [29], Sm_2O_3 in cubic phase is more active and selective than Sm_2O_3 in the monoclinic phase, though both phases have the same basicity. The C-type phase of lanthanide oxides is structurally similar to the defect fluorite lattice except ordering of the oxide ion vacancies. ThO_2-based catalysts prepared by air decomposition/calcination have been reported earlier, and modification of the catalysts with Ca, Ba or Sr improved their OCM

---

* Corresponding author. Tel.: +41 44 632 31 53; fax: +41 44 632 11 63.
E-mail address: baiker@chem.ethz.ch (A. Baiker).

0926-860X/$ – see front matter © 2010 Elsevier B.V. All rights reserved.
doi:10.1016/j.apcata.2010.03.058

performance [30]. However, little information of the effect of doping on the structure was reported. This prompted us to synthesize Ca-substituted ThO_2 catalysts and their Na/K dispersed analogs and to investigate their structural properties and catalytic performance in the oxidative coupling of methane. The catalysts were characterized using nitrogen adsorption, XRD, TEM, TPD, Raman, and EPR spectroscopies. The performance and stability of the catalysts is compared to several reference catalysts. EPR measurements confirm that oxide ion vacancies are likely to play a key role as active sites in the oxidative coupling reaction.

2. Experimental

2.1. Catalyst preparation

Thorium nitrate (Aldrich-Fine Chemicals, 99%), calcium nitrate (Acros Organics, 99+%), sodium nitrate, potassium carbonate, strontium nitrate, magnesium oxide, citric acid, manganese (II) nitrate hydrate (Aldrich-Fine Chemicals, 98%), sodium tungstate (Na_2WO_4, Sigma–Aldrich, 99%) and amorphous SiO_2 were used as received. To prepare $La(NO_3)_3$, La_2O_3 was heated in a small amount of concentrated HNO_3 and evaporated to dryness. α-Al_2O_3 (99.5%; Strem Chemicals), used as inert diluent during methane oxidative coupling in the fixed-bed reactor, was crushed and sieved to obtain the 50–100 μm fraction.

The catalysts were prepared by the citric acid gel method [31]. To prepare ThO_2, $Th_{0.8}Ca_{0.2}O_2$ and Na- or K-modified $Th_{0.8}Ca_{0.2}O_2$ catalysts, stoichiometric amounts of the corresponding salts were dissolved in water and an excess amount (~5 times of the metal salts by weight) of citric acid was added, yielding a transparent solution. The solution was boiled to form a gel after evaporation which was dried at 120 °C. The carbonaceous part in the gel was completely burnt off in the furnace at 700 °C for 15 h and a white colored product was obtained. Repetitive preparation of catalyst batches did not show significant deviation in catalytic results.

The reference catalysts, 5%Sr/La_2O_3 and 5%Li/MgO were prepared following the above procedure. 1.9%Mn–4%Na_2WO_4/SiO_2 was synthesized following the procedure reported by Jiang et al. [32]. In brief, the catalyst was prepared by mixing a slurry of $Mn(NO_3)_2$, Na_2WO_4 and silica gel. After drying, the catalysts were calcined at 800 °C for 8 h, crushed and sieved to obtain 50–100 μm granules.

Safety note: ThO_2-based materials are weakly radioactive and materials should be disposed off according to regulations. Use in the large scale application needs permit from national health authorities.

2.2. Catalyst characterization

Nitrogen physisorption isotherms (adsorption–desorption branches) were measured on a Micromeritics ASAP 2000 instrument at 77 K. Samples were outgassed for 1 h under vacuum at 400 °C before measurement and the specific surface area (SSA) was determined using the BET method.

X-ray diffractograms were recorded on a Siemens D5000 using Cu Kα_1 (λ = 1.54056 Å) radiation in step mode between 20 and 80° 2θ with a step-size of 0.02° and 8 s/step. Metallic Cu was used as an internal standard.

For transmission electron microscopy (TEM), the material was dispersed in ethanol and few drops were deposited onto a perforated carbon foil supported on a copper grid. TEM investigations were performed on a CM30ST microscope (FEI; LaB_6 cathode, operated at 300 kV, point resolution ~2 Å). Particle size was calculated by averaging 25 particles selected randomly.

Raman spectra were recorded with an Ocean Optics QE6500 spectrometer equipped with a fiber optics probe (InPhotonics, RIP-RPB-785) and a 785 nm excitation laser.

ATR-IR measurements were carried out by pressing the powder onto an internal reflection element (ZnSe crystal) in a Bruker Vertex 70 spectrometer. Spectra were taken with a 4 cm^{-1} resolution and consisted of 200 or 400 added scans for the spectrum or background, respectively.

Thermogravimetric (TG) experiments were performed on a Netzsch STA 449 C thermoanalyzer. The exhaust gas was analyzed by an Omnistar (Pfeiffer Vacuum) mass spectrometer connected to the thermoanalyzer by a heated stainless steel capillary. Temperature programmed desorption (TPD) was performed with a flow of 50 mL/min He and a heating rate of 5 K/min to 1130 °C.

Continuous-wave (CW) EPR spectra were acquired on a Bruker Elexsys E500 X-Band Spectrometer with 42 dB attenuation at 25 K (microwave frequency ca. 9.48 GHz) with a modulation amplitude of 4 Gauss. The spectrometer was equipped with a super-high Q resonator (ER 4122 SHQ) and a He-flow cryostat (ESR 910, Oxford Instruments). Spectral simulations of CW EPR powder patterns were done using the Matlab package EasySpin [33].

2.3. Catalytic tests

The reactor set-up was a conventional gas flow system where methane (99.5% PanGas) and oxygen (99.999%, PanGas) were co-fed over the catalyst. The catalyst was placed in a quartz U-tube reactor (ID 4.5 mm) which itself was placed inside a temperature controlled furnace. Typically, 30 mg of catalyst was diluted with 500 mg of α-Al_2O_3 and kept in place between two quartz wool plugs. The quartz wool before the bed acted as a pre-heating zone. Gas flows were regulated by mass flow controllers (Brooks Instrument B. V, model 5850E). The temperature was measured by a thermocouple well on the outer surface of the quartz reactor at the middle of the catalyst bed. Although the catalyst bed was diluted with α-Al_2O_3, the existence of some temperature gradients in the bed cannot be ruled out. Reactions were performed in the temperature range 430–730 °C. The exhaust gas was analyzed using an on-line gas chromatograph with both TCD and FID detectors, which was connected to the reactor with heated (120 °C) stainless steel lines. The GC (Agilent Technologies, model 6890N) was equipped with a CarbonPLOT capillary column which was able to fully separate exhaust gas components such as O_2, CO, CO_2, CH_4, C_2H_4, C_2H_6, C_3H_6, and C_3H_8. Each of the products was calibrated against a calibration gas mixture. A blank run (quartz tube filled with only quartz wool and α-Al_2O_3) showed no conversion at the reaction conditions used. The catalysts after 24 h of reaction are designated as spent catalyst.

The methane conversion and C_{n+} products (ethylene + ethane + propane + propylene) selectivity are defined as:

$$\text{Methane conversion, } X_{CH_4}\ (\%) = \frac{\text{moles of CH}_4 \text{ equivalent of carbon products}}{\text{moles of CH}_4 \text{ in feed}} \times 100$$

$$\text{Selectivity of C}_{n+} \text{ product, } S_{C_{n+}}\ (\%) = \sum \left(\frac{n \times \text{moles of C}_{n+} \text{ products}}{\text{moles of CH}_4 \text{ equivalent of carbon products}} \right) \times 100$$

$$\text{Yield of C}_{n+} \text{ product, } Y_{C_{n+}}\ (\%) = \frac{\text{methane conversion} \times \text{C}_{n+} \text{ selectivity}}{100}$$